Using fluid flow simulations to model microscopic tumor invasion in muscle tissue for radiotherapy treatment

Gregory Buti[1], Ali Ajdari[1], Yen-Lin Chen[1], Christopher P. Bridge[2], Gregory C. Sharp[1], and Thomas Bortfeld[1]

[1]Massachusetts General Hospital and Harvard Medical School, Department of Radiation Oncology, Boston, USA
[2]Massachusetts General Hospital and Harvard Medical School, Athinoula A. Martinos Center for Biomedical Imaging, Charlestown, USA

Abstract
A framework is developed to include the preferred path of microscopic tumor invasion along muscle fibers in radiation target volumes. Following the novel idea that the directionality of muscle fibers inside the muscle can be represented by a flow velocity field, fluid flow simulations are performed with a computational fluid dynamics solver using the finite-elements method. The flow velocity fields are then embedded in a shortest path algorithm to model the microscopic infiltration around the gross tumor. The model assumes that the preferred path of microscopic tumor invasion is along the dominant muscle fiber direction estimated from the velocity field. The method was tested on a sacral chordoma tumor, a malignant tumor originating in the pelvis with suspected microscopic invasion of the gluteal muscles.

1 Introduction

Chondrosarcoma is a type of cancer that originates in cartilage cells and typically develops in bone structures of the pelvis, femur, upper arm, or shoulder blade [1]. One of the major uncertainties in the treatment of chondrosarcomas is how to account for microscopic tumor invasion into the surrounding musculature. It is known that tumor cells encounter greater resistance in the transverse direction of the muscle fiber than in the longitudinal direction [2]. Therefore, to maximize the therapeutic effect, one should use radiation target volumes with more generous margins in the longitudinal direction of the muscle fiber. However, defining such target volumes is a real challenge because CT images have poor soft tissue contrast and therefore cannot provide much intramuscular information. In addition, the typical clinical expansion algorithms that are used to generate radiation target volumes are unable to account for muscle-specific orientation and muscle fiber architecture. As a result, physicians are currently limited to manually delineating target volumes or using expansions along the major anatomical axes, which is an oversimplification of the complex muscle anatomy.
A promising computational approach in the field of biomechanics is the analysis of muscle force generation by representing muscle fibers as an idealized flow of a fluid within the boundaries of the muscle surface. In [3, 4], the equivalence was made between muscle fibers connecting bones through the origin and insertion with an irrotational and incompressible flow between a source and drain. It was shown that the orientation of the vector field from such fluid flow simulations can reproduce the microscopic muscle fiber orientations obtained from the patient's diffusion tensor image, which is a direct representation of the muscle microstructure.
The goal of this study is to combine recent advances in automatic expansion algorithms and fluid flow simulations to create radiation target volumes with local muscle fiber orientation into a single framework. The framework is tested for a sacral chordoma, a type of chondrosarcoma that develops in the sacrum with suspected infiltration in the surrounding gluteal muscles.

2 Materials and Methods

This section presents the framework for obtaining radiotherapy target volumes with muscle fiber information. The main goal is to generate the clinical target volume (CTV), which includes the volume of suspected microscopic tumor invasion. The CTV is obtained as a geometric expansion of the gross tumor volume (GTV), where the GTV-to-CTV expansion is spatially modulated according to the preferred mode of tumor invasion along the muscle fiber direction. The calculation is based on volume delineations of muscles and their corresponding attachment sites (muscle origins and insertions). Here we use a patient, called the *template* patient, with the complete set of delineations available, which serves as the basis for the flow calculations. The results can then be mapped to other different patients, called *target* patients, that do not have attachment delineations available. In short, the workflow consists of (a) performing fluid flow simulations in the template patient for the different gluteal muscles, (b) mapping the flow fields onto the target patient, and (c) generating radiation target volumes by including the mapped flow fields in a shortest path calculation [5]. The first step requires the use of the Finite Element Method (FEM) in a mesh-like geometry as explained below.

2.1 Flow simulation & mesh generation

The flow in a simply-connected domain can be described as a potential flow, through the use of a velocity potential ϕ. Assuming that the flow is both irrotational and incompressible, the Laplacian, ∇^2, of the velocity potential must be zero and the problem reduces to solving a Neumann boundary value

problem for the Laplace equation:

$$\begin{aligned} \nabla^2\phi &= 0, \quad \text{in muscle} \\ \nabla\phi \cdot \mathbf{n} &= 0 \quad \text{on muscle} \end{aligned} \tag{1}$$

$\mathbf{n}$ denotes the vector normal to the muscle surface, so the second equation imposes a zero flux condition at the muscle periphery. Fixed Dirichlet boundary conditions are imposed at the origin and insertion sites in order to simulate a flow between a source (origin) and drain (insertion):

$$\begin{aligned} \phi &= a \quad \text{in origin} \\ \phi &= b \quad \text{in insertion} \end{aligned} \tag{2}$$

with scalar values a and b. Since only the orientation of the potential flow is relevant to our problem, the values for a and b can be arbitrarily chosen as long as $a \neq b$. Finally, the flow velocity field $\mathbf{v}$ is obtained as $\mathbf{v} = \nabla\phi$. Fig. 1 A) gives a schematic overview of the problem statement.
All binary volumetric structures extracted from the patient dicom files were converted into volume meshes in Python. First, the *skimage* marching cubes algorithm is used to find a surface mesh from binary volumetric data. Then, the *pygalmesh* library is used to generate a volumetric tetrahedral mesh from the surface mesh [6], which is used as the domain for the FEM computation (see Fig. 1 B). Eq. (1) is solved using the open-source FEM computing platform FEniCS [7].

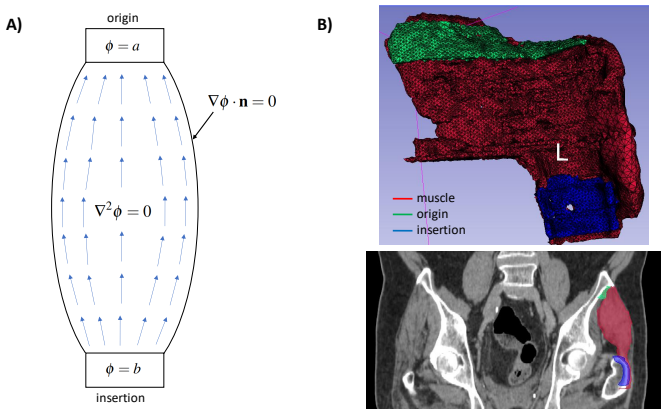

Figure 1: A) Schematic drawing of the Laplacian flow simulation problem. B) Example of the template gluteus medius mesh structures showing the muscle, origin and insertions (top), and associated CT image with structure segmentations (bottom).

2.2 Shortest path calculation & volume generation

A GTV-to-CTV margin can be obtained by using a shortest path calculation with GTV at the origin. Within this framework, the CTV is defined as an iso-distance contour in the 3D shortest distance map. The shortest distance S can be found as a solution to the Eikonal equation [5, 8]:

$$\nabla^\mathsf{T} S \cdot \mathbf{G}^{-1} \cdot \nabla S = 1, \tag{3}$$

where $\mathbf{G}$ is a positive semidefinite tensor of second order, called the Riemann metric tensor, or simply the metric. The metric plays an important role because it models the suspected tumor infiltration distance in a tissue. The relationship between the metric and the velocity field can be established by identifying the orientation of the velocity field as the orientation of greatest distance increase in the space defined by the metric. One way to formalize this relationship between $\mathbf{G}^{-1}$ and $\mathbf{v}$ is by first, creating a 3×3 tensor as the outer product, $\otimes$, of $\mathbf{v}$ with itself and performing a spectral decomposition:

$$\mathbf{v} \otimes \mathbf{v} = Q \cdot \Lambda \cdot Q^{-1}, \tag{4}$$

with Q and Λ the matrices of eigenvectors and eigenvalues, respectively. Second, replacing Λ by a parameterized diagonal matrix $diag(\alpha, 1, 1)$ and defining:

$$\mathbf{G}^{-1} \equiv Q \cdot diag(\alpha, 1, 1) \cdot Q^{-1}. \tag{5}$$

α is a dimensionless free parameter that controls the relative distance increase along the principal eigenvector which, in this context, corresponds to the preference for tumor invasion along the dominant muscle fiber direction.
The shortest path equation was solved using the Python-based fast marching solver HamiltonFastMarching [9].

2.3 Image registration & velocity field transformation

Image registration is used to transform the flow velocity fields from the template patient to the target patient for insertion in (3). Let $\mathbf{v}_1, ..., \mathbf{v}_n$ be the flow velocity fields for a set of n muscle compartments in the template patient. n separate displacement vector fields between the muscle compartment pairs. The transformed flow velocity fields in the target patient are then obtained by multiplying each velocity field by the *inverse* Jacobian matrix J of its associated displacement vector field, $\tilde{\mathbf{v}} = J^{-1} \cdot \mathbf{v}$ [10]. Similarly, the $\mathbf{G}^{-1}$ can be transformed directly according to the tensor transformation rule:

$$\tilde{\mathbf{G}}^{-1} = J^{-1} \cdot \mathbf{G}^{-1} \cdot J^{-\mathsf{T}}. \tag{6}$$

Eq. 6 allows the mapping of velocity fields between different patients by accounting for geometric differences such as differences in size and shape of muscles. Therefore, replacing $\mathbf{G}^{-1}$ by $\tilde{\mathbf{G}}^{-1}$ in (3) enables the calculation of a 3D shortest distance map in the target patient image.
Deformable image registrations between muscles was performed using DIPY (version 1.6.0) [11].

2.4 Patient data

A sacral chordoma patient, with manual delineations of the gluteus maximus, gluteus minimus and gluteus medius is used as a template image for obtaining muscle fiber information. The origin and insertion sites for all muscles of the template patient were delineated by an experienced radiation oncologist in our institution. Another sacral chordoma patient without origins/insertions available was used as a target image to generate the CTV. The hip bones, which act as

an impermeable barrier to tumor infiltration, were autosegmented on the CT image using TotalSegmentator (version 2.0.5) [12].

3 Results

This section presents the results of the flow simulation in the template patient, followed by a comparison of the CTVs in the target patient with and without the inclusion of preferential models of tumor invasion.

3.1 Flow simulations

Fig. 2 shows the flow velocity fields in the template patient, overlayed on the CT image for the various gluteal muscles. As displayed, the FEM obtained smooth vector fields that can be mapped to the target patient.

3.2 CTVs

Fig. 3 compares the CTVs in the patients with and without muscle fiber orientation. The reference CTVs are defined as volumes with a 10 mm margin around the GTV in non-muscle tissue and larger margins of 20 mm and 30 mm in the gluteal muscles. The fiber-specific CTVs were generated by specifying a value of $\alpha > 1$ in the gluteal muscles and $\alpha = 1$ in the other tissues. As α increases, the model increases its preference for muscle invasion along the muscle fiber direction. We choose values for α equal to 4.0, and 9.1 because these specific values for α correspond to the standard CTV ranges mentioned earlier.
Significant differences in the shape of the CTVs are observed, especially as the CTV margins become more anisotropic. The difference between the reference CTV and the muscle fiber CTV was quantified using the 95% Hausdorff distance (HD95). The HD95 was 7.6 mm, and 13.9 mm for the (10 / 20) mm and (10 / 30) mm CTVs, respectively. This means that our proposed method has the potential to significantly impact current CTV delineation standards.

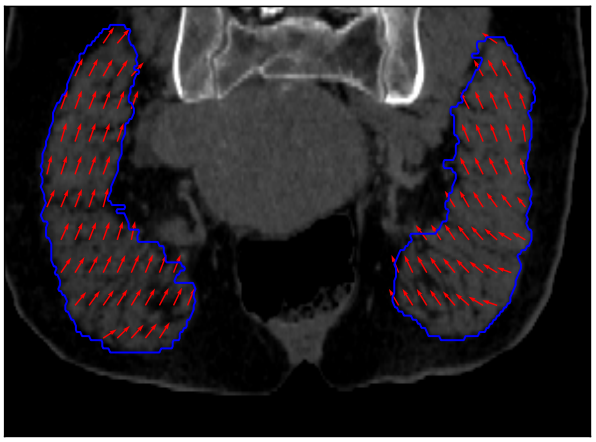

(a) Gluteus maximus

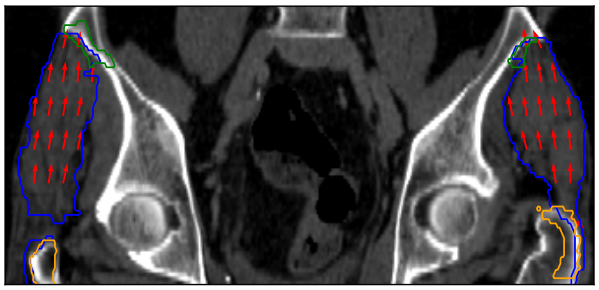

(b) Gluteus medius

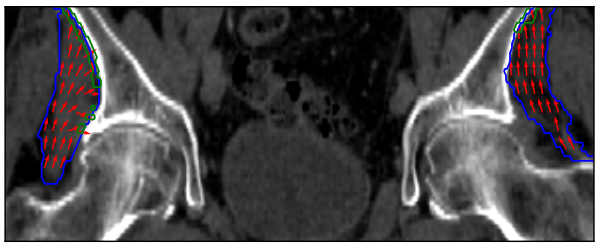

(c) Gluteus minimus

Figure 2: The flow velocity field obtained through Laplacian flow simulations are depicted by the red arrows within the (a) gluteus maximus, (b) gluteus medius and (c) gluteus minimus muscles. The flow vectors are assumed to be representative of the muscle fiber direction.

4 Discussion

In radiation therapy, the goal is to deliver a therapeutic dose to the CTV so that all tissues suspected of harboring tumor cells are treated. Currently, for chondrosarcoma treatments, the CTV is defined as a geometric expansion of the GTV by specifying a uniform margin in the muscle compartment. However, such an oversimplified approach does not take into account the mode of tumor invasion along the muscle fibers. As a result, tumorous tissue may be undertreated or radiation may be delivered to areas that are potentially tumor-free.
This study develops a computational method to improve the target volume definition for tumors with spread patterns along certain predefined structures such as skeletal muscles. Spread patterns were derived from Laplacian flow simulations to obtain patient-specific muscle fiber information. The Laplace equation is a fundamental equation in physics as it arises in a number of phenomena such as gravitational theory, electrostatics, fluid mechanics, and the heat equation. In this context, Laplace's equation is used to simulate a laminar flow that is representative of the directionality of the muscle fibers inside the muscle. Formally, potential flows governed by Laplace's equation are solutions to the time-independent Navier–Stokes equations for viscous (low Reynolds numbers), incompressible and irrotational fluids [4]. Realistic muscle fiber trajectories can be obtained by imposing different types of boundary conditions. First, a constant inflow and outflow was assumed at the origin and insertion sites, and second, a zero flux condition at the muscle periphery prevented muscle fibers from leaking through the outer muscle

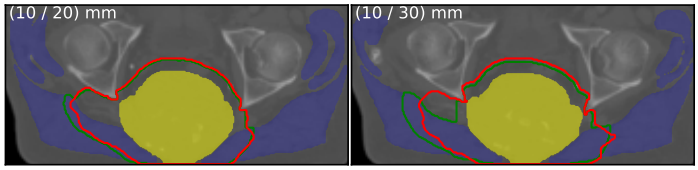

(a) Axial slice.

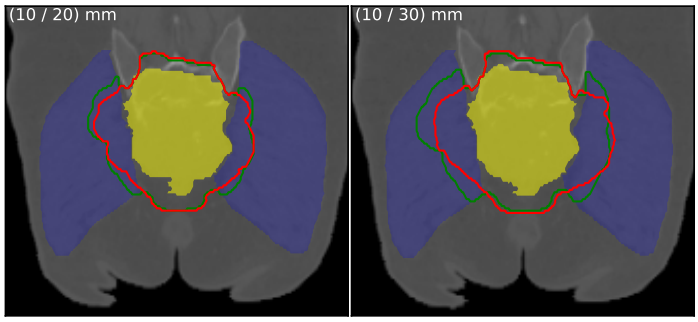

(b) Coronal slice.

Figure 3: Comparison of the standard CTV with margins of (10 / 20) mm and (10 / 30) in non-muscle / muscle tissue in green, against the model-based CTVs in red, overlayed on the patient CT image. The GTV and muscle masks are shown in yellow and blue, respectively.

surface .

Once the flow fields have been computed with the FEM, insertion into the shortest path algorithm enables the generation of radiation target volumes. The shortest path map models the preferential invasion for miscroscopic tumor invasion in the tissues surrounding the gross tumor. Here, the flow velocity is equivalent to the presumed tumor infiltration distance along its principal direction.

A limitation of the current implementation is that muscle insertions are not currently delineated in clinical routine. Therefore, the decision was made to manually delineate origins and insertions in a single patient CT image, which served as a template to provide muscle fiber information. Automatic segmentation of insertion sites may be an interesting avenue for future research to further personalize the model.

Future research will focus on validating the model, and introducing tumor-specific effects such as the displacement of origin and insertion sites by the gross disease and disruptions of muscle fibers. In prospective setting, model validation requires the use of DTI. Alternatively, retrospectively, the orientation and magnitude of the flow velocity fields can be informed by areas of recurrence after treatment.

5 Conclusion

This study presents a novel framework for incorporating the preferred path of tumor invasion into the clinical target volume for radiotherapy treatments. The directionality of tumor invasion was estimated using fluid flow simulations to obtain realistic muscle fiber trajectories. The method has the potential to improve the consistency and accuracy of the clinical target volume, thereby reducing the physician's time burden.

References

[1] A. Gazendam, S. Popovic, N. Parasu, et al. "Chondrosarcoma: A Clinical Review". *Journal of Clinical Medicine* 12.7 (Mar. 2023), p. 2506. DOI: 10.3390/jcm12072506.

[2] L. Beunk, K. Brown, I. Nagtegaal, et al. "Cancer invasion into musculature: Mechanics, molecules and implications". *Seminars in Cell & Developmental Biology* 93 (Sept. 2019), pp. 36–45. DOI: 10.1016/j.semcdb.2018.07.014.

[3] G. G. Handsfield, B. Bolsterlee, J. M. Inouye, et al. "Determining skeletal muscle architecture with Laplacian simulations: a comparison with diffusion tensor imaging". *Biomechanics and Modeling in Mechanobiology* 16.6 (June 2017), pp. 1845–1855. DOI: 10.1007/s10237-017-0923-5.

[4] J. Varvik, T. F. Besier, and G. G. Handsfield. "Computational fluid dynamics simulations for 3D muscle fiber architecture in finite element analysis: Comparisons between computational fluid dynamics and diffusion tensor imaging". *International Journal for Numerical Methods in Biomedical Engineering* 37.12 (Sept. 2021). DOI: 10.1002/cnm.3521.

[5] G. Buti, A. Ajdari, K. Hochreuter, et al. "The influence of anisotropy on the clinical target volume of brain tumor patients". *Physics in Medicine & Biology* 69.3 (Jan. 2024), p. 035006. DOI: 10.1088/1361-6560/ad1997.

[6] N. Schlömer. *pygalmesh: Python interface for CGAL's meshing tools*. 2021. DOI: 10.5281/ZENODO.5564818.

[7] I. A. Baratta, J. P. Dean, J. S. Dokken, et al. *DOLFINx: The next generation FEniCS problem solving environment*. en. 2023. DOI: 10.5281/ZENODO.10447666.

[8] T. Bortfeld and G. Buti. "Modeling the propagation of tumor fronts with shortest path and diffusion models—implications for the definition of the clinical target volume". *Physics in Medicine and Biology* 67.15 (July 2022), p. 155014. DOI: 10.1088/1361-6560/ac8043.

[9] J.-M. Mirebeau and J. Portegies. "Hamiltonian Fast Marching: A Numerical Solver for Anisotropic and Non-Holonomic Eikonal PDEs". *Image Processing On Line* 9 (Feb. 2019), pp. 47–93. DOI: 10.5201/ipol.2019.227.

[10] G. B. (B. Arfken, H.-J. Weber, and F. E. Harris. *Mathematical methods for physicists : a comprehensive guide*. 7th ed. Elsevier, 2013.

[11] E. Garyfallidis, M. Brett, B. Amirbekian, et al. "Dipy, a library for the analysis of diffusion MRI data". *Frontiers in neuroinformatics* 8 (2014), p. 8.

[12] J. Wasserthal, H.-C. Breit, M. T. Meyer, et al. "TotalSegmentator: Robust Segmentation of 104 Anatomic Structures in CT Images". *Radiology: Artificial Intelligence* 5.5 (Sept. 2023). DOI: 10.1148/ryai.230024.